Article

# Displacement induced off-on fluorescent biosensor targeting IDO1 activity in live cells

Jing Jia, Huilin Wen, Sibo Zhao, Lancheng Wang, Haishi Qiao, Haowen Shen, Ziyi Yu, Bin Di, Li-Li Xu, and Chi Hu

*Anal. Chem.*, **Just Accepted Manuscript** • DOI: 10.1021/acs.analchem.9b03387 • Publication Date (Web): 12 Nov 2019

# Displacement induced off-on fluorescent biosensor targeting IDO1 activity in live cells

Jing Jia,[†,‡] Huilin Wen,[¶] Sibo Zhao,[§] Lancheng Wang,[§] Haishi Qiao,[§] Haowen Shen,[†,‡] Ziyi Yu,[¶] Bin Di,[*,†,‡] Lili Xu,[*,†,‡] and Chi Hu[*,§]

†*Jiangsu Key Laboratory of Drug Design and Optimization, China Pharmaceutical University, Nanjing 210009, China.*

‡*Key Laboratory of Drug Quality Control and Pharmacovigilance, China Pharmaceutical University, Ministry of Education, Nanjing 210009, PR China.*

¶*State Key Laboratory of Materials-Oriented Chemical Engineering, College of Chemical Engineering, Nanjing Tech University, 30 Puzhu South Road, Nanjing 211816, PR China.*

§*Department of Pharmaceutical Engineering, School of Engineering, China Pharmaceutical University, Nanjing 211198, PR China.*

E-mail: dibin@cpu.edu.cn; 1620174420@cpu.edu.cn; chihu@cpu.edu.cn

**Abstract**

We show how the macrocyclic host cucurbit[8]uril (CB[8]) and a fluorescent dye form a biosensing ensemble while its cavity simultaneously traps tryptophan, the upstream substrate of IDO1 enzymes, therefore providing a label-free method to monitor the activity of IDO1 in real time. Incubation of malignant HeLa and HepG2 cells overexpressing IDO1 with the associative biosensor resulted in its spontaneous uptake and a fluorescence switch-on response *in situ*, which can be traced to the displacement of tryptophan from CB[8] upon IDO1-catalyzed oxidation. The results, for the first time, establish a supramolecular sensing concept for the detection of intracellular enzymatic

activity in live cells, thus allowing direct cell-based analysis and inhibitor screening compatible with commercial instruments including microplate reader, fluorescent microscopy and flow cytometry.

# Introduction

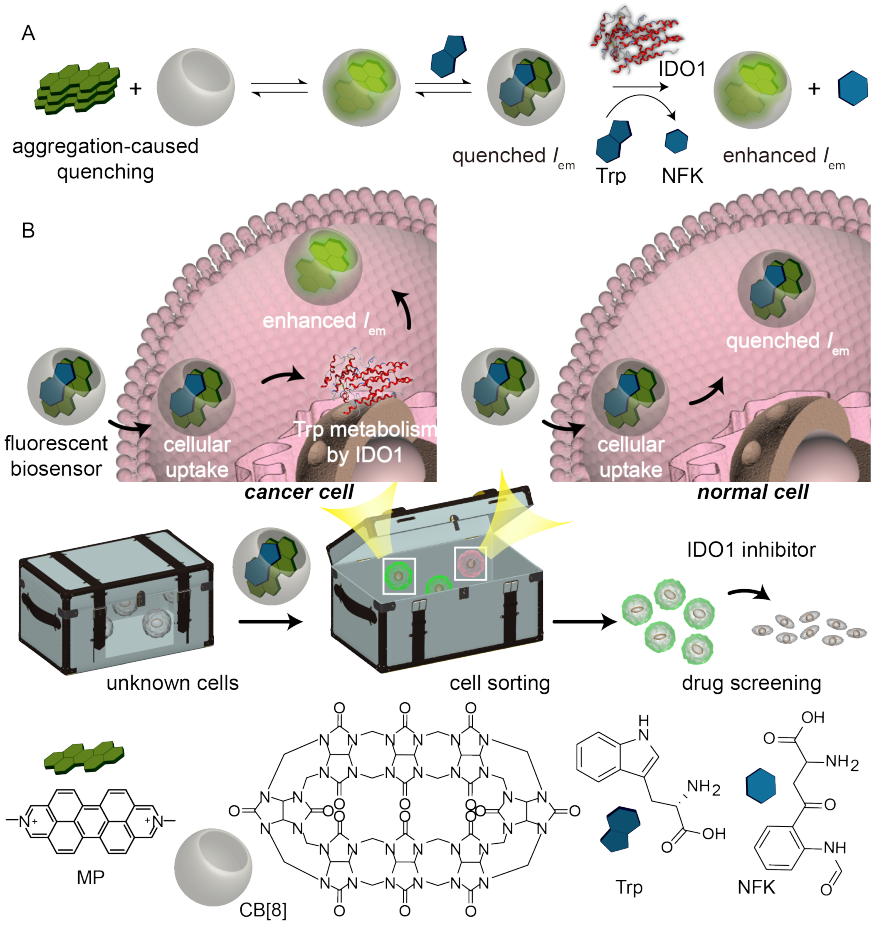


Figure 1: (A) Fluorescent biosensor for intracellular IDO1 activity is self-assembled with the macrocyclic host CB[8] and dicationic dye MP. Metabolism of Trp into NFK through IDO1-catalyzed reaction is coupled to a change in the amount of Trp-bound and free biosensor. (B) The associative biosensor (MP · Trp)⊂CB[8] displays quenched fluorescence in normal cells. In cancer cells where IDO1 enzymes are overexpressed, (MP · Trp)⊂CB[8] is converted to MP⊂CB[8], resulting in enhanced fluorescence.

Present therapies fail many patients as tumors escape immune rejection through the evolution of various tactics to evade, subvert and reprogram innate and adaptive immu-

nity.[1] One such immunosuppression mechanism that has emerged with broadly useful appeal is mediated by the cytosolic enzyme indoleamine 2,3-dioxygenase 1 (IDO1), which acts in immunometabolism and inflammatory programming through catalyzing the oxidation of tryptophan (Trp) into downstream *N*-formylkynurenine (NFK). Small-molecule inhibitors of IDO1 have been demonstrated to empower the efficacy of cytotoxic chemotherapy, radiotherapy and immune checkpoint therapy, with a set of mechanistically distinct compounds including indoximod, epacadostat and navoximod (NLG-919) being evaluated in clinical trial.[2] Moreover, the expression of IDO1 is specifically induced by the inflammatory stimuli from the tumor microenvironment with reports on its overexpression in several tumors (lung, hepatocellular, colorectal, cervical and ovarian, *etc.*) instead of healthy tissues, making it a potential biomarker for the sorting of cancer cells.[3]

Methods for monitoring the biocatalytic activity of IDO1 are indispensable for the elucidation of reaction mechanism, the screening of inhibitors, and the analysis of malignant cells.[4] Antibodies have been employed to modify proteins and peptides with high specificity, at the expense of arduous synthetic procedures, added costs and frequently non-reproducible activity.[5] Other techniques like high-performance liquid chromatography (HPLC) suffer from drawbacks in their requirements for sample preparation and long acquisition times, which restrict their applicability in high-throughput analyses.[6] An absorbance assay was described by Takikawa *et al.* on account on the yellow pigment derived from kynurenine (the downstream product of NFK) after reacting with *p*-dimethylaminobenzaldehyde (*p*-DMAB), however, this approach could only afford indirect sensing of the IDO1 activity.[7] Direct quantification of NFK has been achieved through reaction with piperidine[8] or commercialized NFK GreenScreen$^{TM}$ kit[9] to produce a fluorophore, however, these methods require relatively harsh derivatization conditions that are not suitable for live cell studies.

Supramolecular tandem assays based on the sensing ensemble composed of an indicator dye and a macrocyclic host have been introduced to provide cheap, simple to use and amenable to high-throughput screening of enzyme activities such as protease,[10] phos-

phatase,[11] and neuraminidase.[12] For instance, Biedermann and co-workers reported an associative chemosensor by cucurbit[8]uril (CB[8])-dimethyldiazaperopyrenium dication (MP) complexes, and used it to monitor enzymatic reactions including peroxidases, dehydrogenases, laccases, peptidases, esterases, phosphatases, penicillinase, and $\beta$-galactosidase in bulk solutions.[13] Nau and co-workers presented a chemosensing ensemble consisting of the macrocycle p-sulfonatocalix[4]arene and the fluorescent dye lucigenin, and used it as an indicator displacement assay for the detection of the uptake of bioorganic analytes by live cells.[14] To the best of our knowledge, however, supramolecular tandem assays have not been transferred to study enzymatic activity in cellular systems.[15,16]

We now present a supramolecular tandem assay that associates with Trp, thereby allow the real-time monitoring of its IDO1-catalyzed conversion into NFK in live cells on account of the highly specific host-guest recognition, which provides a sizable tolerance towards competitive binders such as salts, metabolites and proteins present in biological samples.[17,18] As shown in Figure 1, the associative biosensor is obtained by the spontaneous inclusion of MP into the cavity of the macrocycle CB[8] to form a binary complex MP$\subset$CB[8] with green fluorescence.[19,20] The residual cavity inside CB[8] allows for the subsequent binding of Trp to form a heteroternary complex (MP $\cdot$ Trp)$\subset$CB[8], which is accompanied by net fluorescence quenching.[21–23] Importantly, the non-covalent and reversible host-guest complexation responds instantaneously to the change in Trp concentration and translates it directly into alteration of the ratio of emissive (Trp-free) and non-emissive (Trp-bound) biosensors, thus providing a change in the measurable emission intensity ($I_{em}$).

# Experimental

***Chemicals and Materials:*** CB[8][24] and MP[25] were prepared according to literature procedures. Trypothan was purchased from Macklin Biochemical (China). NFK was purchased from Nanjing Dernor Pharmaceutical Technology (China). Recombinant human

IFN-$\gamma$ was purchased from Sino biological (China). NLG919, IDO inhibitor 1 and BMS-986205 were purchased from Selleck (China). Twenty-nine compounds with purity over 95.0% were purchased from Topscience (China). All other materials were purchased from Aladdin Reagent Company and used as received. Deionized water was obtained using a Millipore Synergy UV purification system (18.2 M$\Omega$ cm$^{-1}$).

A SpectraMax i3x (Molecular Devices) microplate reader was utilized to measure UV absorbance and fluorescence emission spectra. Experiments were performed in triplicate. An Olympus IX73 microscope was employed to record fluorescent microscopy images. BD Accuri C6 instrument was used to perform flow cytometry.

***IDO1 activity in bulk solution:*** An assay medium (100 μL) was prepared with phosphate buffer (50 mM, pH 6.5), ascorbic acid (40 mM, neutralized with an equimolar amount of NaOH), methylene blue (10 μM), catalase (150 μg mL$^{-1}$) and Trp (100 μM). To the assay medium was added crude IDO1 (20 μL) and the mixture was incubated at 37 °C. The supernatant (15 μL) was collected at predetermined time intervals and MP⊂CB[8] (5 μM, 700 μL) was added for fluorescence measurement (Ex: 441 nm, Em: 510 nm). Inhibitors were dissolved in dimethyl sulfoxide at a concentration of 10 mM and diluted to the desired concentration in the assay medium prior to adding IDO1.

For HPLC quantification of kynurenine, 50% volume of trichloroacetic acid (30% in water) was added after the indicated time and the mixture was incubated for 30 min at 50 °C. After centrifugation for 10 min (10,000 ×g), the supernatants were directly analyzed with HPLC (Ultramate 3000, Thermo) at the wavelength of 280 nm on a Hypersil GOLD C18 column (5 μm, 250 × 4.6 mm, Thermo). The mobile phase was prepared with 9% acetonitrile, 0.1% acetic acid and 0.1% trifluoroacetic acid.

***IDO1 activity in live cells:*** For testing IDO1 activity with fluorescence spectroscopy, HeLa and HepG2 cells were cultured in fresh medium and pre-incubated with different concentrations of IFN-$\gamma$ in a 12-well plate at time 0 h. After 24, 48, 72 or 96 h, to the culture medium (15 μL) was added MP⊂CB[8] (5 μM, 700 $\mu$L) and the mixture was subjected to

fluorescence measurement using a microplate reader.

For fluorescent microscopy visualization, cells were pre-incubated with IFN-$\gamma$ (50 ng $mL^{-1}$). After 24 h, the cells were washed with PBS and incubated in Hanks' Balanced Salt Solution (HBSS) containing (MP · Trp)⊂CB[8] (10 μM) and MP⊂CB[8] (40 μM) at 37 °C under 5% $CO_2$ for 30 min. Subsequently, the cells were washed with PBS and imaged under fluorescent microscopy.

For FACS analysis, cells were pre-incubated with IFN-$\gamma$ (50 ng $mL^{-1}$). After 24 h, the cells were trypsinized and incubated in HBSS containing (MP · Trp)⊂CB[8] (10 μM) and MP⊂CB[8] (40 μM) at 37 °C under 5% $CO_2$ for 1 h. Subsequently, the cells were collected by centrifugation, resuspended in PBS, and subjected to FACS. Notably, ternary (MP · Trp)⊂CB[8] was used for fluorescent microscopy imaging and FACS measurement, where cells were directly analyzed; otherwise binary MP⊂CB[8] was employed in cell culture medium or bulk solutions where Trp is abundantly present.

***Western blot:*** HeLa and HepG2 cells were pre-incubated with different concentrations of IFN-$\gamma$. After 24 h, cells were lysed in a buffer containing Tris-HCl (50 mM, pH 7.4), NaCl (150 mM), sodium vanadate (1 mM), Nonidet P-40 (1%) and protease inhibitors (Selleck, China). The cell lysate was centrifuged at 10,000 ×g, and the supernatant was collected and diluted with loading buffer before separation by SDS-PAGE. The protein was transferred to a polyvinylidene difluoride membrane (Roche, USA), where IDO1 antibody (1:1000, Cell Signaling Technology, China) was used to detect the protein followed by HRP-conjugated secondary antibody and the ECL reagent kit (Tanon, China). The images were collected using an Alpha Innotech FluorChem FC2 imaging system (Gel Doc$^{TM}$ EE imager, USA).

***Inhibitor screening in live cells:*** Cells were pre-incubated with IFN-$\gamma$ (50 ng $mL^{-1}$) and IDO1 inhibitors for 24 h. Subsequently, to the culture medium (15 μL) was added MP⊂CB[8] (5 μM, 700 $\mu$L) and the mixture was subjected to fluorescence measurement using a microplate reader.

***Absorbance assay:*** To the culture medium was added 50% volume of trichloroacetic

acid (30% in water) and the mixture was incubated for 30 min at 50 °C. After centrifugation for 10 min at 10,000 ×g, *p*-DMAB (100 µL, 2% in glacial acetic acid) was added to the supernatant and the mixture was vortexed for 3 min at 1,200 rpm before measurement.

# Results and discussion

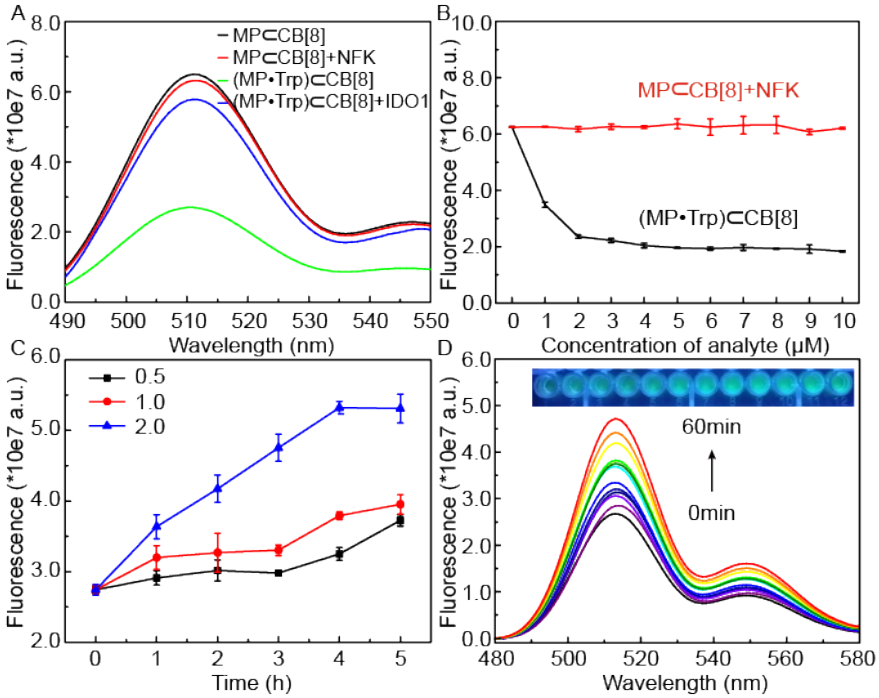


Figure 2: (A) Fluorescence spectra for IDO1-catalyzed (2.0 µg mL$^{-1}$, crude) oxidation of Trp (1.7 µM) as reported by the associative biosensor MP⊂CB[8] (5 µM). (B) Normalized fluorescence of MP⊂CB[8] at 510 nm with varying concentrations of Trp and NFK. (C) Reaction progress curves under different IDO1 concentrations (0.5-2.0 µg mL$^{-1}$, crude). (D) Development of fluorescence spectra as a function of reaction time in the presence of 3.0 µg mL$^{-1}$ crude IDO1 enzymes. Measurements were carried out in 96-well kinetic mode at 37 °C with instrument readings taken at 5-min intervals; inset shows the photographs of the corresponding reaction mixture under UV light (365 nm) illumination.

The hydrophobic fluorophore MP exhibits a high propensity towards aggregation and unspecific adsorption in aqueous solutions, which are detrimental for most applications.[25] The formation of host-guest inclusion complex with CB[8] prevents MP from $\pi$-$\pi$ stacking and dramatically increase its fluorescence intensity, as shown in Figure 2A. Binding of the second

guest Trp induces a quenching of the MP⊂CB[8] fluorescence, which increases with the concentration of Trp introduced (Figure 2B). On the contrary, almost identical fluorescence intensity was recorded in the presence of NFK (1.7 μM), suggesting negligible interaction between NFK and the associative biosensor.[26]

Stability of the biosensor in the assay medium for IDO1, which contains ascorbic acid, catalase and methylene blue in phosphate buffer, was investigated. Low micromolar concentration of Trp is sufficient to obtain reasonable resolution in $I_{em}$, demonstrating high sensitivity of the system. Compatibility of this supramolecular approach to IDO1 activity monitoring is confirmed as shown in Figure 2C, where the variation of the enzyme concentration yielded the expected proportionality of the initial rates. With low enzyme concentration such as 0.5 μg $mL^{-1}$, prolonged incubation of Trp with IDO1 is necessary to obtain a measurable conversion ratio and therefore a reasonably significant increase in fluorescence intensity. A robust, time-dependent increase in fluorescence signal was generated within 1 h of reaction as shown in Figure 2D. Different affinities of the enzyme substrate and product towards the binary complex MP⊂CB[8] are imperative to enable a change in the measurable $I_{em}$. The magnitude of the intensity change is a function of the concentration, binding affinity ($K_a$) and quenching efficiency ($Q_E$) of the Trp-NFK couple. As IDO1-catalyzed oxidation of Trp takes place in the aryl anchor and forms a formyl group in its vicinity, increased steric hindrance is expected to be imposed on heteroternary complex formation with CB[8], leading to $K_a$(Trp) > $K_a$(NFK) and an increase in $I_{em}$. The above observations confirm that the biosensor does not interfere with the enzymatic activity and remains stable under the experimental conditions.

Applicability of the biosensors to live-cell measurements was demonstrated in HeLa and HepG2 cells.[27] Although photophysical properties of the associative reporter are diminished as expected owing to the presence of large amounts of competitive salts, nutrients, and other biomolecules, they remain at a sufficiently high level to retain a response to the target analyte Trp.[28] As shown in Figure 3, without cytokines such as interferon-γ (IFN-γ, abundant

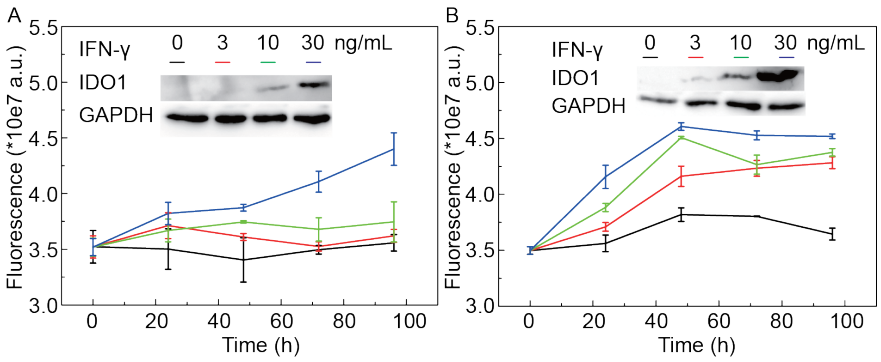


Figure 3: Kinetic profiles of IDO1-catalyzed oxidation of Trp into NFK in (A) HeLa and (B) HepG2 cells in the presence of various concentrations of IFN-$\gamma$, as was monitored by the biosensor MP⊂CB[8] (5 μM) in the cell culture medium. IFN-$\gamma$ induced expression of IDO1 at 24 h is shown by western blot in the inset image.

in the tumor microenvironment) in the cell culture medium to promote the expression of IDO1, minimum $I_{em}$ was reported as Trp present in the culture medium maintained the biosensor in its quenched form, *i.e.*, (MP · Trp)⊂CB[8]. In the presence of IFN-$\gamma$ to induce the intracellular expression of IDO1, expected increase in $I_{em}$ was observed as a function of Trp conversion in a time-resolved manner. Notably, a more pronounced increase in $I_{em}$ was observed for HepG2 cells in comparison to HeLa cells, presumably because of the higher IDO1 expression level of the former, which is also supported by the inset western blot images and previous literature reports.[7] While fluorescence intensity showed a continuous increase in HeLa cells under all IDO1 concentrations examined within the 96 h time window, incubation times longer than 48 h led to relatively smaller fluorescence recoveries in HepG2 cells, likely related to proteolysis of the enzyme to its constituent amino acids including Trp. The slight fluorescence recovery without IFN-$\gamma$ to promote the expression of IDO1 in HepG2 cells is likely on account of other enzymes capable of catalyzing the oxidation of Trp, such as tryptophan 2,3-dioxygenase (TDO) and indoleamine 2,3-dioxygenase 2 (IDO2).

Nevertheless, the above results encouraged the implementation of the (MP · Trp)⊂CB[8] reporter to monitor IDO1 activity in live-cell measurements.[29,30] As shown in the optical images in Figure 4A, both MP⊂CB[8] and (MP · Trp)⊂CB[8] showed spontaneous uptake

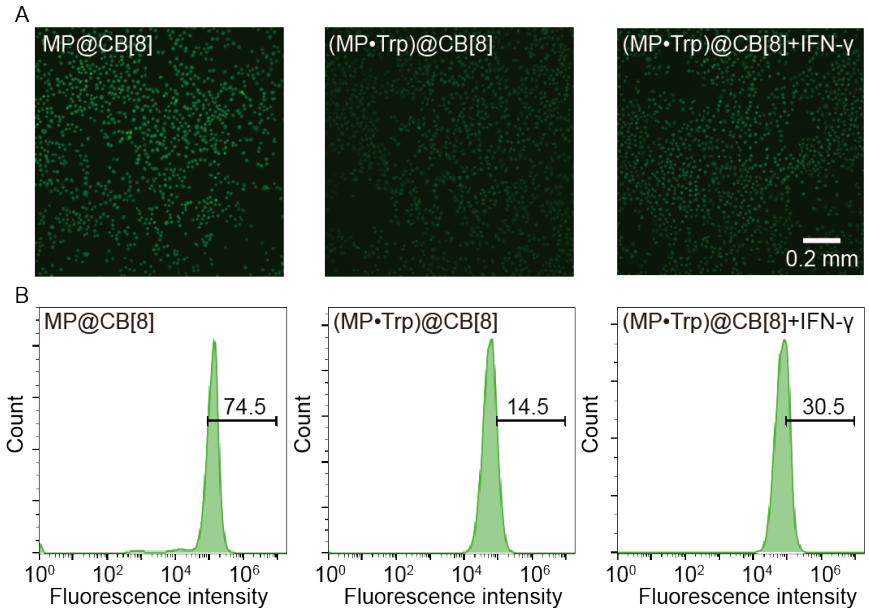


Figure 4: (A) Fluorescence images and (B) FACS histograms of HeLa cells incubated with MP⊂CB[8] (left), (MP · Trp)⊂CB[8] (middle), and (MP · Trp)⊂CB[8] with IFN-γ (right).

into HeLa cells, where the latter exhibited quenched fluorescence on account of the net effect.[14,31] In the presence of IFN-γ, however, a switch-on fluorescence response was readily observed, thereby confirming the dissociation of (MP · Trp)⊂CB[8] and thus the presence of active IDO1. Instead of only physically adsorbed on the cell membrane surface or approachable in the outer cell membrane layer, the fluorescence enhancement again confirms the cellular uptake of the reporter system, which is readily accessible to the cytosolic IDO1 enzymes.[32] As shown in Figure 4B, the activity of IDO1 enzymes inside HeLa cells can also be quantitatively analyzed by fluorescence-activated cell sorting (FACS). Upon incubation with (MP · Trp)⊂CB[8] and subsequent FACS analysis, approximately 30.5% of the cells pre-treated with IFN-γ fall within the box compared to the IDO1-negative cells (14.5%). Thus, for the first time, a fluorescent sensor-based route toward probing IDO1 activity in cell-based measurements is reported, which avoids need for pretreatment such as labelling or use of labeled secondary antibody.

It is noteworthy that an incubation of 30-60 min was required for the cellular uptake of the biosensor before live-cell measurements, otherwise the collected cells did not show

any fluorescence, further confirming stability of the host-guest complex in cytoplasm as the displacement process occurs within milliseconds.[13,33] The surprising finding that the associative biosensor remains operational inside live cells can be ascribed to a combination of three main characteristics of the host-guest system. Firstly, the dicationic dye MP binds CB[8] with a high affinity ($K_a > 10^6$ $M^{-1}$) to form a chemically robust binary complex, which provides a readily accessible and photostable system with emission in the visible region.[34,35] Secondly, Trp quenches the fluorescence of MP⊂CB[8] very efficiently in the assay medium (by a $Q_E$ of 58% at only 0.3 eq. of the analyte), thus ensuring a sizable response upon the depletion of Trp by IDO1. Thirdly, the MP⊂CB[8] complex exhibits a specific molecular recognition of Trp instead of its downstream metabolite NFK.

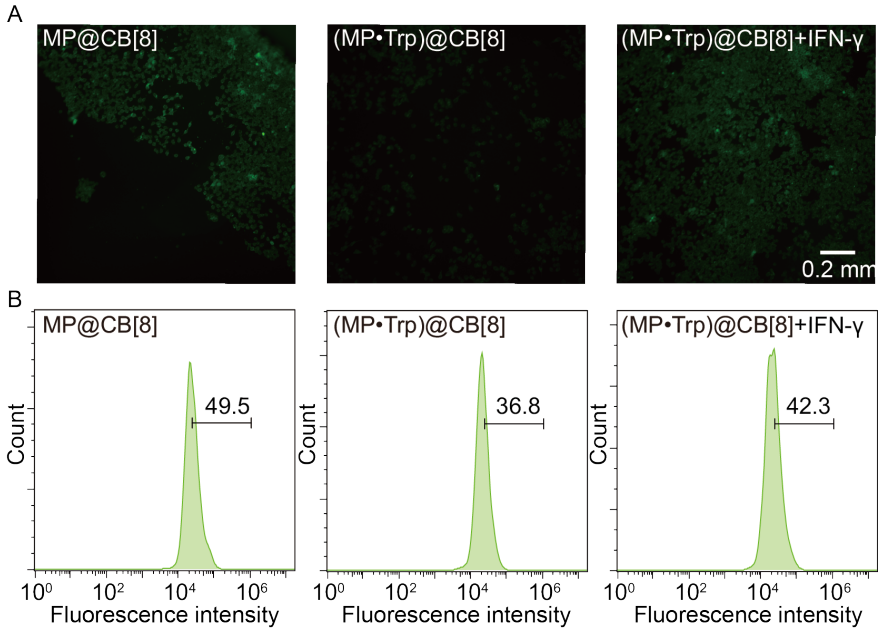


Figure 5: (A) Fluorescence images and (B) FACS histograms of HepG2 cells incubated with MP⊂CB[8] (left), (MP · Trp)⊂CB[8] (middle), and (MP · Trp)⊂CB[8] with IFN-γ (right).

Cellular analysis was also performed on HepG2 cells, where the cells pre-incubated with IFN-γ showed significantly enhanced cellular fluorescence with almost identical intensity as those stained with MP⊂CB[8] (Figure 5). The observed switch-on fluorescence, as opposed to a simple quenching, requires the liberation of the second guest Trp from the host-guest ensemble, thus demonstrating the presence of active IDO1 enzymes to deplete Trp. Therefore,

the (MP · Trp)⊂CB[8] biosensors can be conveniently employed to stain live cells for direct visualization of their intracellular IDO1 expression. Notably, the fluorescence enhancement varied depending on the cell line, and a more drastic increase was observed in HepG2 cells in comparison to HeLa cells under otherwise the same conditions, indicating more significant enzymatic activity in the former cell line. This observation is consistent with results from cell culture medium as shown in Figure 3, likely on account of the relatively low extent of IDO1 induction in HeLa cells by IFN-$\gamma$. The good agreement between results obtained from three independent commercial instruments, *i.e.*, microplate reader, fluorescent microscopy and FACS suggests reliability, applicability and reproducibility of the biosensor system.

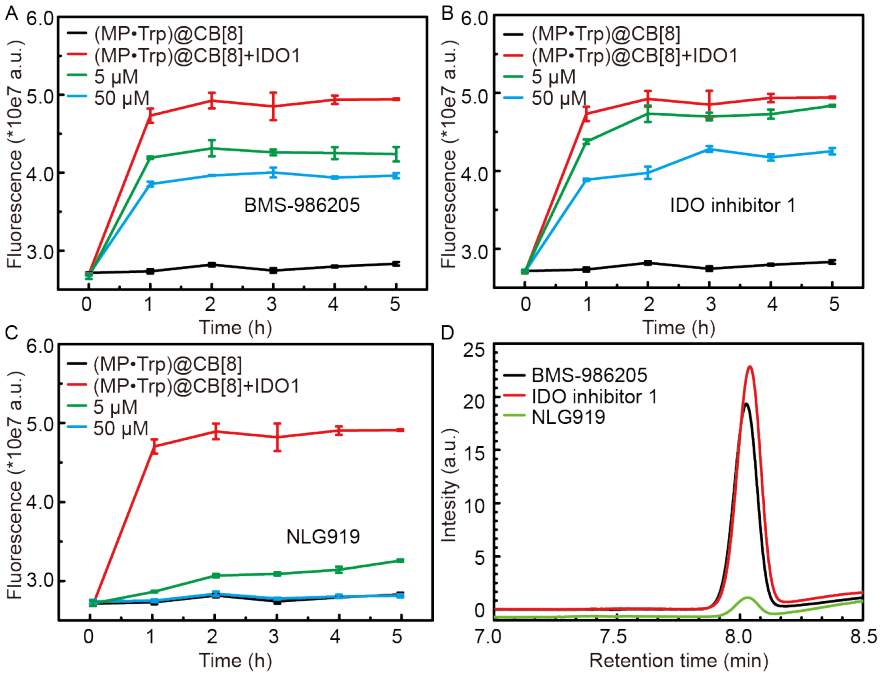


Figure 6: Inhibition profiles for (A) BMS-986205, (B) IDO inhibitor 1, and (C) NLG919. Assays were carried out in 96-well plates using 5 μM MP⊂CB[8]. Data points are the means ± SD for triplicate samples carried out simultaneously in the same microplate. (D) HPLC quantification of kynurenine at 5 h in samples treated with the three inhibitors at a concentration of 50 μM.

From a pharmacologic standpoint, inhibition of IDO1 activity has attracted vast interest for small-molecule drug development. In an effort to extend our biosensor system to the screening of IDO1 inhibitors, the dynamic change of enzymatic activity in bulk solutions

with or without inhibitor treatment is investigated as shown in Figure 6. In line with intuition, quenched fluorescence was reported by MP⊂CB[8] in the presence of three clinical or pre-clinical IDO1 inhibitors (BMS-986205, IDO inhibitor 1 and NLG919) with various efficiency, *i.e.*, NLG919>BMS-986205>IDO inhibitor 1. To benchmark our associative biosensor, inhibition of IDO1 activity was compared to HPLC quantification of kynurenine, the downstream product of the resulting NFK. As shown in Figure 6D, both methods yielded very similar results, where NLG919 showed a most prominent efficiency of approximately 101% at a concentration of 50 μM after 5 h.

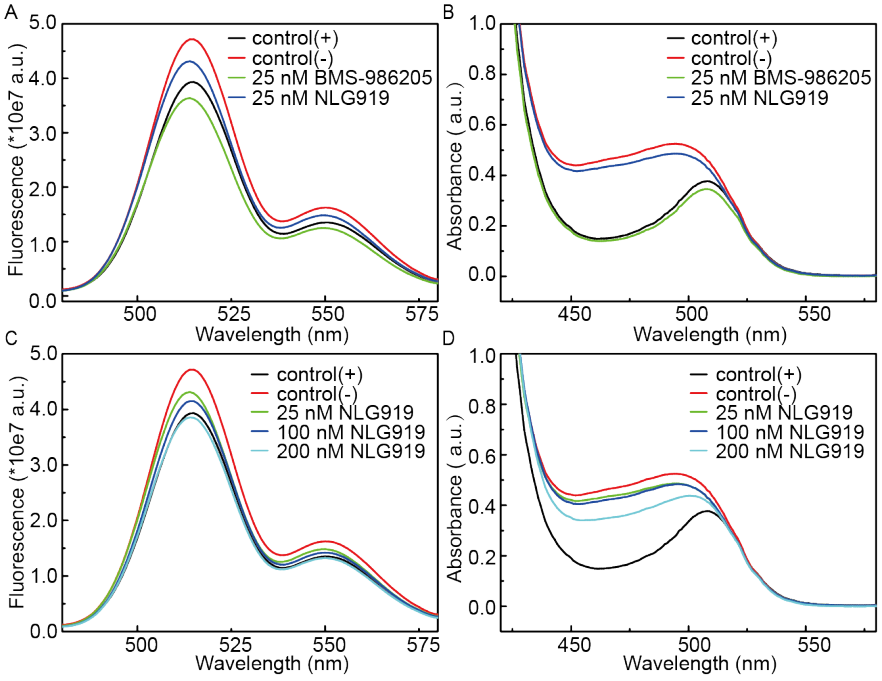


Figure 7: Inhibition assay of IDO1 by BMS-986205 and NLG919 in HepG2 cells, as reported by (A) the biosensor MP⊂CB[8] (5 μM) and (B) *p*-DMAB (1 wt%) using the cell culture medium. Dose-response curves of NLG919 at different inhibitor concentrations, as reported by (C) the biosensor MP⊂CB[8] and (D) *p*-DMAB.

As potent inhibition of purified enzymes could be greatly reduced in proteomes through reaction with many proteins and metabolites in the cellular environment, *In vitro* studies were performed in HepG2 cells to further confirm selective inhibition of IDO1. Negative-control reactions without added inhibitors and positive-control reactions without added IFN-$\gamma$ to induce IDO1 expression were included to set low and high boundaries for fluorescence signals,

respectively. As shown in Figure 7A, while NLG919 shows the most significant inhibition of IDO1 in bulk solutions, it performs less well in live cells with an inhibitor efficiency of 39%, in comparison to the value of 124% for BMS-986205. Although the *in vivo* therapeutic efficiency of the inhibitors are composite effects that depend on various factors such as bioavailability, live-cell based fluorescent bioassay in principle offers the possibility for monitoring IDO1 activity *ex vivo* under different treatment conditions. A conventional method, where kynurenine was derivatized by reaction with *p*-DMAB prior to absorbance measurement at 480 nm, was also employed to determine IDO1 activity. As shown in Figure 7B, an inhibitor efficiency of 105% and 11% was calculated for BMS-986205 and NLG919, respectively. This (slight) inconsistency may result because of the different analytes the two methods are based on, *i.e.*, our fluorescent biosensors response to the upstream substrate Trp directly, whereas the conventional absorbance assay characterizes the downstream product of the IDO1-catalyzed reaction.

Next, a library of 29 compounds were interrogated in a 96-well plate format for molecules which selectively inhibit IDO1 activity in HepG2 cells, and two novel hits were successfully identified. As shown in Figure 8A, the assay performance was consistent across plates, with robust fluorescence intensity and signal-to-noise ratio suitable for high-throughput screening. From this screen, two primary hits were identified as compounds 1 and 5 (10 μM) that reduced the fluorescence signal of MP⊂CB[8] by 89% and 64% relative to positive-control reactions, respectively. The highly-sensitive probe can also be incorporated into secondary screens to rapidly rule out false-positive primary hits, where activity of the hit compounds were evaluated in dose-dependent assay (Figure 8B and C). This assay revealed that compound 1 showed a gradually augmented efficiency in blocking IDO1 activity with concentrations increasing from 3.2-10 μM, whereas the activity of compound 5 was lost at concentrations lower than 10 μM. To validate the biosensor system, we compared inhibitor efficiency obtained with the fluorescence assay and with the standard HPLC method (Figure 8D). Values measured by HPLC were 92% and 85% for compound 1 and 5, respectively,

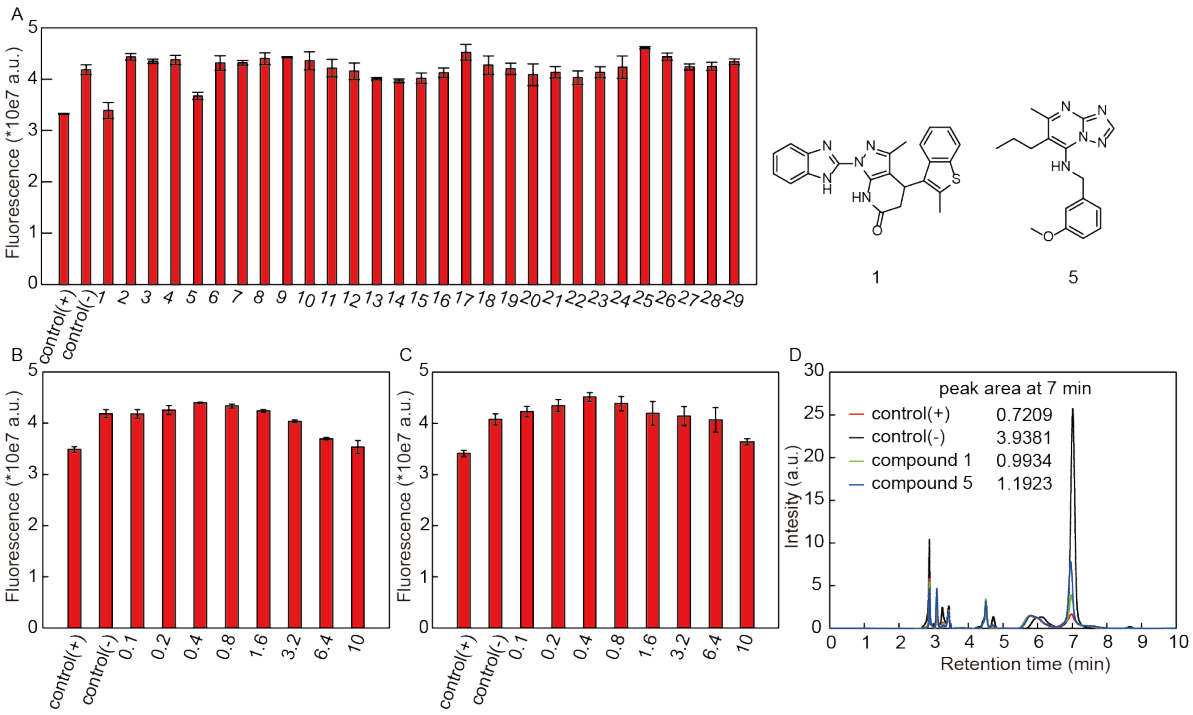


Figure 8: IDO1 inhibitor screening in HepG2 cells using MP⊂CB[8]. (A) Results for a library of 29 compounds at a concentration of 10 μM. Dose-dependent assay for (B) compound 1 and (C) compound 5. (D) HPLC quantification of kynurenine in samples treated with compound 1 and 5 (10 μM).

in good agreement with those obtained with our fluorescence assay, therefore ruling out false-positive and nonselective hits.

# Conclusions

A supramolecular tandem assay has been developed by exploiting the heterogeneous guest inclusion capability of CB[8] to monitor the enzymatic activity of IDO1 *in situ* in live cells, normally not achievable with standard techniques. Compatibility of the method with commercial instruments including microplate reader, fluorescent microscopy and FACS was demonstrated in malignant HeLa and HepG2 cells, where the enzymatic conversion of Trp was followed in real time and recognized as a putative biomarker for the sorting of cancer cells. The highly sensitive biosensors also provide label-free drug screening in a high-throughput format, allowing for nanomolar identification of potent IDO1 inhibitors that would escape

detection when observing their fluorescence/absorption alone. We believe that the associative biosensing strategy can find a wide range of applications in cell-based analysis and small molecule screen for novel IDO1 inhibitors, bypassing the need to synthesize specific antibodies for immunoassays or construct nanotechnological sensing systems.

## Associated content

The Supporting Information is available free of charge on the ACS Publications website at DOI: xxx. Experimental details for the optimization of the fluorescence assay and screening assay, the expression of IDO1 proteins, and cell culture conditions are listed; quality of the assay is also evaluated.

## Acknowledgement

This work was supported by the National Key R&D Program of China (2018YFC0807402), the National Natural Science Foundation of China (NSFC 81803485, 81573386), and the Natural Science Foundation of Jiangsu Province (BK20170731).

## References

(1) Chen, D. S.; Mellman, I. *Nature* **2017**, *541*, 321–330.

(2) Prendergast, G. C.; Malachowski, W. P.; DuHadaway, J. B.; Muller, A. J. *Cancer Res.* **2017**, *77*, 6795–6811.

(3) Godin-Ethier, J.; Hanafi, L.-A.; Piccirillo, C. A.; Lapointe, R. *Clin. Cancer Res.* **2011**, *17*, 6985–6991.

(4) Liu, Y.; Perez, L.; Gill, A. D.; Mettry, M.; Li, L.; Wang, Y.; Hooley, R. J.; Zhong, W. *J. Am. Chem. Soc.* **2017**, *139*, 10964–10967.

(5) Gu, K.; Xu, Y.; Li, H.; Guo, Z.; Zhu, S.; Zhu, S.; Shi, P.; James, T. D.; Tian, H.; Zhu, W.-H. *J. Am. Chem. Soc.* **2016**, *138*, 5334–5340.

(6) Tian, Z.; Ding, L.; Li, K.; Song, Y.; Dou, T.; Hou, J.; Tian, X.; Feng, L.; Ge, G.; Cui, J. *Anal. Chem.* **2019**, *91*, 5638–5645.

(7) Takikawa, O.; Kuroiwa, T.; Yamazaki, F.; Kido, R. *J. Biol. Chem.* **1988**, *263*, 2041–8.

(8) Tomek, P.; Palmer, B. D.; Flanagan, J. U.; Sun, C.; Raven, E. L.; Ching, L.-M. *Eur. J. Med. Chem.* **2017**, *126*, 983–996.

(9) Seegers, N.; van Doornmalen, A. M.; Uitdehaag, J. C. M.; de Man, J.; Buijsman, R. C.; Zaman, G. J. R. *J. Biomol. Screen.* **2014**, *19*, 1266–1274.

(10) Ghale, G.; Ramalingam, V.; Urbach, A. R.; Nau, W. M. *J. Am. Chem. Soc.* **2011**, *133*, 7528–7535.

(11) Liu, Y.; Lee, J.; Perez, L.; Gill, A. D.; Hooley, R. J.; Zhong, W. *J. Am. Chem. Soc.* **2018**, *140*, 13869–13877.

(12) Liu, W.; Gómez-Durán, C. F. A.; Smith, B. D. *J. Am. Chem. Soc.* **2017**, *139*, 6390–6395.

(13) Biedermann, F.; Hathazi, D.; Nau, W. M. *Chem. Commun.* **2015**, *51*, 4977–4980.

(14) Norouzy, A.; Azizi, Z.; Nau, W. M. *Angew. Chem. Int. Ed.* **2015**, *54*, 792–795.

(15) Yin, T.; Zhang, S.; Li, M.; Redshaw, C.; Ni, X.-L. *Sensors Actuat. B-Chem.* **2019**, *281*, 568–573.

(16) Zhou, Y.; Gao, L.; Tong, X.; Li, Q.; Fei, Y.; Yu, Y.; Ye, T.; Zhou, X.-S.; Shao, Y. *Anal. Chem.* **2018**, *90*, 13183–13187.

(17) de Vink, P. J.; Briels, J. M.; Schrader, T.; Milroy, L.-G.; Brunsveld, L.; Ottmann, C. *Angew. Chem. Int. Ed.* **2017**, *56*, 8998–9002.

(18) Wei, L.; Wang, X.; Li, C.; Li, X.; Yin, Y.; Li, G. *Biosens. Bioelectron.* **2015**, *71*, 348–352.

(19) Ni, X.-L.; Chen, S.; Yang, Y.; Tao, Z. *J. Am. Chem. Soc.* **2016**, *138*, 6177–6183.

(20) Biedermann, F.; Rauwald, U.; Cziferszky, M.; Williams, K. A.; Gann, L. D.; Guo, B. Y.; Urbach, A. R.; Bielawski, C. W.; Scherman, O. A. *Chem. Eur. J.* **2010**, *16*, 13716–13722.

(21) Hirani, Z.; Taylor, H. F.; Babcock, E. F.; Bockus, A. T.; Varnado, C. D.; Bielawski, C. W.; Urbach, A. R. *J. Am. Chem. Soc.* **2018**, *140*, 12263–12269.

(22) Samanta, S. K.; Moncelet, D.; Briken, V.; Isaacs, L. *J. Am. Chem. Soc.* **2016**, *138*, 14488–14496.

(23) Hu, C.; Ma, N.; Li, F.; Fang, Y.; Liu, Y.; Zhao, L.; Qiao, S.; Li, X.; Jiang, X.; Li, T.; Shen, F.; Huang, Y.; Luo, Q.; Liu, J. *ACS Appl. Mater. Interfaces* **2018**, *10*, 4603–4613.

(24) Kim, J.; Jung, I.-S.; Kim, S.-Y.; Lee, E.; Kang, J.-K.; Sakamoto, S.; Yamaguchi, K.; Kim, K. *J. Am. Chem. Soc.* **2000**, *122*, 540–541.

(25) Basuray, A. N.; Jacquot de Rouville, H.-P.; Hartlieb, K. J.; Kikuchi, T.; Strutt, N. L.; Bruns, C. J.; Ambrogio, M. W.; Avestro, A.-J.; Schneebeli, S. T.; Fahrenbach, A. C.; Stoddart, J. F. *Angew. Chem. Int. Ed.* **2012**, *51*, 11872–11877.

(26) Shcherbakova, E. G.; Zhang, B.; Gozem, S.; Minami, T.; Zavalij, P. Y.; Pushina, M.; Isaacs, L. D.; Anzenbacher, P. *J. Am. Chem. Soc.* **2017**, *139*, 14954–14960.

(27) Tian, D.; Li, F.; Zhu, Z.; Zhang, L.; Zhu, J. *Chem. Commun.* **2018**, *54*, 8921–8924.

(28) Sinn, S.; Spuling, E.; Bräse, S.; Biedermann, F. *Chem. Sci.* **2019**, *10*, 6584–6593.

(29) Kubánková, M.; López-Duarte, I.; Bull, J. A.; Vadukul, D. M.; Serpell, L. C.; de Saint Victor, M.; Stride, E.; Kuimova, M. K. *Biomaterials* **2017**, *139*, 195–201.

(30) Liu, Y.; Duan, W.; Song, W.; Liu, J.; Ren, C.; Wu, J.; Liu, D.; Chen, H. *ACS Appl. Mater. Interfaces* **2017**, *9*, 12663–12672.

(31) Zhang, Y.-M.; Liu, J.-H.; Yu, Q.; Wen, X.; Liu, Y. *Angew. Chem. Int. Ed.* **2019**, *58*, 10553–10557.

(32) Mao, W.; Mao, D.; Yang, F.; Ma, D. *Chem. Eur. J.* **2019**, *25*, 2272–2280.

(33) Hennig, A.; Bakirci, H.; Nau, W. M. *Nat. Methods* **2007**, *4*, 629–632.

(34) Biedermann, F.; Nau, W. M. *Angew. Chem. Int. Ed.* **2014**, *53*, 5694–5699.

(35) Zhang, Q.; Deng, T.; Li, J.; Xu, W.; Shen, G.; Yu, R. *Biosens. Bioelectron.* **2015**, *68*, 253–258.

# Graphical TOC Entry